Available online at www.sciencedirect.com
SCIENCE DIRECT®
Composites: Part A 36 (2005) 1518–1524
composites
Part A: applied science and manufacturing
www.elsevier.com/locate/compositesa

Polyethylene/keratin fiber composites with varying polyethylene crystallinity

J.R. Barone*

USDA/ARS/ANRI/EQL, BARC-West, Bldg. 012, Rm. 1-3, 10300 Baltimore Avenue, Beltsville, MD 20705, USA

Received 25 June 2004; revised 28 January 2005; accepted 24 February 2005

Abstract

Short-fiber reinforced composites are made from keratin fibers obtained from poultry feathers and polyethylenes of varying crystallinity. The chemical nature of the polymer and fiber is kept constant and the molecular architecture of the polymer is varied. It is found that low crystallinity polyethylenes are reinforced by keratin fibers but high crystallinity polyethylenes are not. The keratin fibers inhibit crystallinity in low crystallinity polyethylenes but enhance crystallinity in high crystallinity polyethylenes. Microscopy shows increased adhesion between the fibers and the polymer for the more amorphous polyethylenes. A model is presented that describes composite properties as a function of fiber properties and matrix crystallinity.

Keywords: A. Polymer-matrix composites; A. Fibers; B. Mechanical properties; D. Thermal analysis

1. Introduction

There has been much recent work devoted to the use of agricultural fibers, particularly cellulosic fibers derived from plants, in the reinforcement of commodity thermoplastics such as polyethylene (PE) [1–3] and polypropylene (PP) [4–7]. Agricultural fibers are interesting materials to use for the reinforcement of polymers because they are usually of lower density than inorganic fibers, environmentally friendly, and relatively easy to obtain [8]. It is anticipated that the fibers would not contribute to the wear of polymer processing equipment and may not suffer from size reduction during processing, both of which occur when inorganic fibers or fillers are used. Although the absolute property increase when using organic fibers is not anticipated to be nearly as high as inorganic fibers, the specific properties are anticipated to be high owing to the much lower density of the organic fibers [4].

Commodity thermoplastics like polyethylene and polypropylene are semi-crystalline materials. Both materials have glass-transition temperatures (T_g) much less than room temperature and crystalline melting temperatures (T_m) much higher than room temperature. At room temperature, there is a crystalline fraction that can bear load and an amorphous fraction that is mobile and adds 'toughness'. Therefore, semi-crystalline polymers have a range of properties depending on the amount of crystallinity. These properties can be further enhanced through the use of fibers or fillers.

The key to successful enhancement of polymers with fibers of higher modulus or strength is to achieve good polymer/fiber interaction [9]. During processing in the melt state, the molten polymer should spread over and adhere to the fiber creating a strong adhesive bond. However, for this to happen there must be chemical compatibility between the fiber and polymer. Cellulosic agricultural fibers and glass fibers are predominantly hydrophilic in chemical nature. This makes them chemically incompatible with the hydrophobic polyethylene or polypropylene. Therefore, a 'coupling agent', must be used to increase interactions between the fiber and polymer [2,8,10–12]. Feather keratin, a protein fiber, has about 60% hydrophobic amino acids in the amino acid sequence, with the balance being hydrophilic amino acids [13]. So it can be expected that there will be some compatibility between polyethylene or polypropylene and feather keratin fibers. Agricultural fibers are polymeric and therefore it is possible to graft polymers to the surface of the fibers through suitable

* Fax: +1 301 504 5992.
E-mail address: baronej@ba.ars.usda.gov.

1359-835X/$ - see front matter © 2005 Elsevier Ltd. All rights reserved.
doi:10.1016/j.compositesa.2005.03.006

interactions, such as grafting methyl methacrylate to keratin fibers derived from chicken feathers [14] or wool [15]. Recently, Bullions et al. [16] used maleic anhydride-modified PP to increase PP/keratin feather fiber interactions.

When using semi-crystalline polymers as the matrix material for short-fiber reinforced composites, a 'trans-crystalline' layer may develop at the fiber/polymer interface [11,17]. The fiber surface serves as a nucleation site for polymer crystals and the crystals that form at the fiber surface are different from the crystals formed in the bulk polymer. This means that the polymer volume immediately surrounding the fibers has properties different from the bulk polymer. The trans-crystallinity can be affected by fiber type, shear deformation at the fiber/polymer interface, and the cooling rate after processing. The cooling rate after processing has been studied recently for carbon fibers in polyether ether ketone (PEEK) [18] and for cellulose fibers in PP [11,19]. If the volume fraction of fibers, ϕ_f, is high, the trans-crystalline region becomes the bulk and the matrix properties are dominated by the properties of the trans-crystalline material [20–22].

In this paper, keratin feather fiber of 0.1 cm length is incorporated into polyethylenes of varying crystallinity at a constant 20 wt% fiber loading. In addition, the fiber loading is varied and the polymer matrix kept constant to show the effect on composite matrix crystallinity. The properties are assessed and described as a function of polymer crystallinity to note how much applied load is carried by the crystals and how much is carried by the fibers. Scanning electron micrographs of the fracture surfaces denote fiber/polymer interactions and fiber orientation. Thermal analysis shows crystallinity differences in the trans-crystalline layer and the bulk.

2. Experimental

2.1. Keratin feather fiber

Keratin feather fiber is obtained from Featherfiber® Corporation (Nixa, MO) using a process patented by the USDA [23]. The feather fiber is semi-crystalline and has a constant diameter of approximately 5 μm and a density of 0.89 g/cm^3 [24]. More detailed description of feather fiber can be found elsewhere [25–27].

Fibers of 0.1 cm length are made by grinding feather fiber using a Retsch ZM 1000 centrifugal grinder. The rotational velocity of the instrument is 15,000 rpm and contains a torque feedback so as to not feed in too much material and overload the motor. The fiber is fed slowly to avoid motor overload and to minimize frictional heating of the instrument and the fiber.

2.2. Composite preparation

The polymer matrix materials are all commercially available polyethylenes. The properties of the polyethylenes are listed in Table 1. Composites are prepared by first adding PE into a Brabender mixing head set at 150 °C and rotating at 50 rpm. Immediately after adding PE, 20 wt% (weight percent) feather fiber is added into the mixing head. The total sample weight of each composite is 40 g, which represents a degree of fill of 70% of the total volume of the mixing head. The melt temperature is monitored independently. The polymer controls all achieve melt temperatures of ca. 170 °C and the composites all achieve melt temperatures of ca. 185 °C. The total mixing time for each sample is 15 min.

Table 1
PE samples and properties

PE	Source	M_w (g/mol)	M_w/M_n	MFI (g/10 min at 190 °C)	ρ_p (g/cm^3)
LDPE LD133A	Dow	N/A	N/A	0.22	0.923
LLDPE 2045	Dow	110,000	3.77	1.00	0.920
LLDPE 2037	Dow	N/A	N/A	2.50	0.934
HDPE HD5502SA	BP	171,100	27.6	0.20	0.954
HDPE HD7760	Exxon	N/A	N/A	0.06	0.952

Following mixing, each sample is sandwiched between Teflon-coated aluminum foil and pressed into three thin sheets in a Carver Press Autofour/30 Model 4394 at 160 °C, 133,446 N for 18 s. The film is then removed and cooled under an aluminum block until it reaches room temperature. After pressing, each thin film is inspected to note feather fiber dispersion. Previous work shows that pressing does not affect fiber dispersion [24,27]. Good dispersion is observed in all cases.

To prepare samples for testing, the three thin sheets are cut into quarters, stacked on top of each other, sandwiched between Teflon-coated aluminum foil, and pressed in the Carver Press at 160 °C and 8896 N for 2–3 min. After pressing, the films are air cooled until they reach room temperature. This results in plates approximately 0.3 cm in thickness. Type IV dogbone samples for testing according to ASTM D638 are machined from the plates.

To study the effect of thermal processing on the composites and polymers, two of the polymers, a low crystallinity (LD133A) and a high crystallinity (HD7760) PE are annealed after air cooling. Annealing is performed in a convection oven for 24 h. After annealing, the oven is turned off and the sample allowed to cool to room temperature, which takes about 3 hours. Both HD7760 and LD133A are annealed at a temperature of 0.99 T_m. This allows the most change to the microstructure over a given period of time without re-melting the molded plates as annealing proceeds.

2.3. Composite testing

Composite samples are allowed to sit at ambient conditions for 1 week before testing. Uniaxial tensile

testing is performed using a Com-Ten Industries 95 RC Test System. The applied test speed is 2.5 cm/min. Four samples of each composite are tested. Elastic modulus, E, and peak stress, σ_p, i.e. the maximum stress value of the stress–strain curve, are reported.

2.4. Thermal analysis

The thermal properties of the polymers and composites are assessed using differential scanning calorimetry (DSC). A TA Instruments DSC 910s is used according to the procedures outlined in ASTM D3417 and D3418. Sample sizes of ca. 5 mg are used in a N_2 atmosphere. The first heating cycle proceeds from 30 to 200 °C at 10 °C/min. The first heating cycle is followed by a cooling cycle from 200 back down to 20 °C. The cooling rate cannot be controlled. The heater simply shuts off and the DSC cell cools to 30 °C. Although there may be some variation in the cooling step from sample to sample, the room temperature was always the same (20 °C) so it is assumed that the cooling steps are similar. A second heating cycle then proceeds from 30 to 200 °C. Peak assignments and areas are determined according to the ASTM procedures. Each sample is run three times and accuracy of the melting temperatures is found to be within 0.4%, i.e. a few tenths of a degree.

The first heating cycle yields information about the state of the polymer as a function of processing conditions, therefore, these results are reported henceforth. The heat of fusion of the first heating cycle, $\Delta Q_{m,1}$, and the melting temperature during the first heating cycle, $T_{m,1}$, are determined. The crystalline fraction of each polymer and composite is determined from the DSC results using

$$X_1 = \frac{\Delta Q_{m,1}}{\Delta Q_f(1 - m_f)} \quad (1)$$

where ΔQ_f is the theoretical heat of fusion of 100% crystalline PE, $\Delta Q_f = 290$ J/g [28], and m_f is the mass fraction of fiber. Joseph et al. [11] determined the crystallinity of polypropylene composites in a similar manner.

3. Results and discussion

3.1. Thermal properties of polymers and composites

For brevity, the DSC results of LD133A and HD7760 are presented as examples of 'low crystallinity' and 'high crystallinity' behavior, respectively. Table 2 contains $T_{m,1}$ and X_1 for each polymer and composite. Fig. 1 shows the first heating cycle for LD133A polymer and 20 wt% 0.1 cm fiber composite. In general, the presence of the fibers affects the state of crystallinity in the PE matrix. For LD133A, it is observed that $T_{m,1}$ of the composite is lower than $T_{m,1}$ of the polymer. In addition, a second smaller melting peak appears at about 140 °C. This would indicate that there are two populations of LDPE crystals in the polymer composite after processing. Upon cooling and going through the second DSC heating cycle, the smaller melting peak at ca. 140 °C disappears, i.e. the bimodal crystal distribution disappears.

Table 2
Results of DSC first heating cycle

PE	$T_{m,1}$ (°C) pol	X_1 pol ($X_{1,p}$)	$T_{m,1}$ (°C) comp	X_1 comp ($X_{1,m}$)	ρ_m (g/cm^3)
LDPE LD133A	113	0.45	112	0.37	0.911
LLDPE 2045	123	0.44	123	0.39	0.914
LLDPE 2037	128	0.52	127	0.57	0.940
HDPE HD5502SA	132	0.69	131	0.71	0.972
HD7760	132	0.71	130	0.77	0.963
LD133A-a	114	0.44	114	0.44	0.922
HD7760-a	135	0.72	135	0.82	0.980

To investigate the smaller, higher temperature $T_{m,1}$ peak (referred to as $T'_{m,1}$) of the LDPE composites further, DSC is performed on 0.1 cm fiber composites as a function of fiber mass fraction, m_f. The composites of variable m_f are prepared the same way as the 20 wt% composites. Fig. 2 shows the evolution of the $T'_{m,1}$ peak as a function of increasing fiber content. Plotted are the values of $T'_{m,1}$ and $\Delta G'_{m,1}$ as a function of fiber mass fraction. As fiber fraction increases, so does the peak area and position. Meanwhile, the larger $T_{m,1}$ peak remains relatively unchanged with increasing m_f. This indicates that the overall amount of crystallinity is increasing in the LD133A composites as the fiber content increases. The composites have a population of larger crystals residing closer to the fibers as indicated by the $T'_{m,1}$ peak results. The number of larger crystals closer to the fibers is increasing with fiber content.

Fig. 3 shows the DSC results for the first heating cycle of HD7760 and the 20 wt% 0.1 cm fiber composite. Again, the composite has a lower $T_{m,1}$ than the polymer. In the case of HD7760, there is no indication that a second population of crystals exists, as there is no second peak in the composite DSC. Table 2 shows that $T_{m,1}$ of the composites, except for LLDPE 2045, is lower than $T_{m,1}$ of the polymer. The general trend would indicate that the polymer matrices in the composites have thinner, easier melting crystals than the bulk polymers when processed in a similar manner [22].

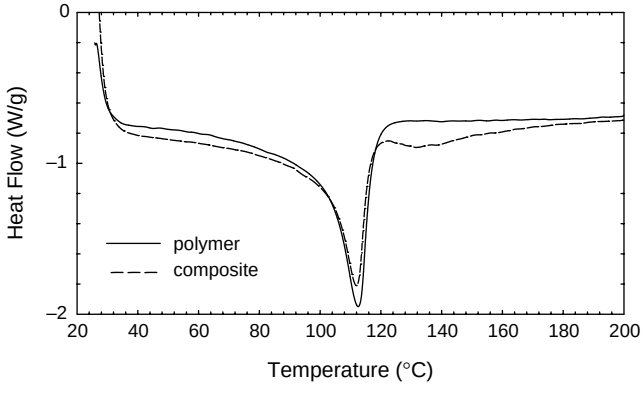

Fig. 1. DSC first heating curve for LD133A and 20 wt% composite.

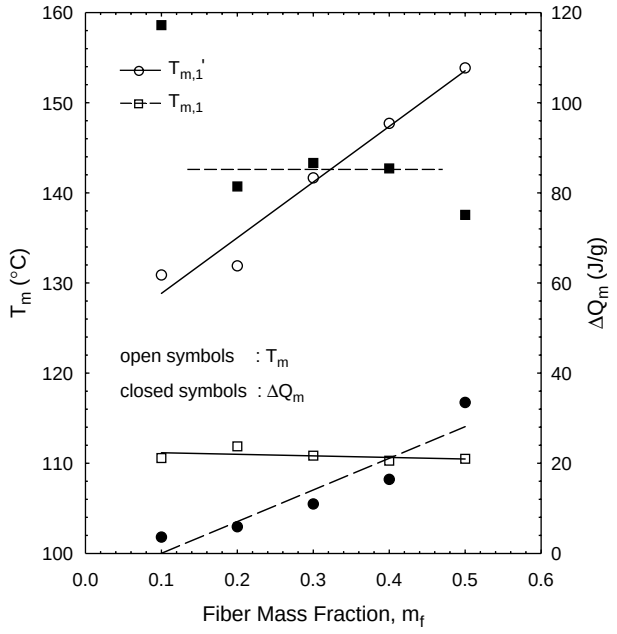

Fig. 2. Change in $T'_{m,1}$ peak of LD133A composites with increased fiber mass fraction, m_f. Melting temperature, T_m, and area under curve, ΔQ_m are shown.

What is interesting about the crystalline fraction, X_1, data in Table 2 is that the addition of fibers suppresses crystallinity in the two lowest density PE's but enhances crystallinity in the higher density PE's. The density values of LD133A and LLDPE 2045 infer more branching in these polymers over the other PE's. Joseph et al. [11] see an increase in the crystallinity of PP with addition of sisal fibers and explain this as extra nucleating surfaces for PP crystals. These researchers also note the increase of crystallinity with increased fiber weight fraction. The results presented here show that having increased surface area for crystal nucleation, i.e. adding fibers, is not enough to enhance crystallinity. PP is a linear chain and is highly crystalline so it would be analogous to the higher crystallinity or density samples used in the current study. What this shows is that the architecture of the chain affects the interaction of the polymer with the fiber, even though all of the polymers have the same chemical composition of polyethylene. A transition seems to occur at around $X_1 \sim 0.5$, where the presence of the fibers no longer suppresses crystallinity but enhances it.

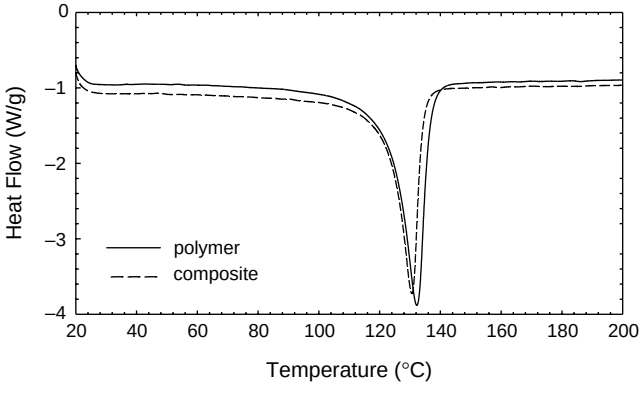

Fig. 3. DSC first heating curve for HD7760 and 20 wt% composite.

3.2. Effect of annealing on polymer crystallinity

Fig. 4 shows the DSC first heating curves for LD133A and HD7760 after annealing for 24 h at 0.99 T_m. Table 2 also contains the $T_{m,1}$ and X_1 values, labeled as LD133A-a and HD7760-a. Annealing LD133A composite samples increases the crystallinity of the polymer matrix back to the value of the pure polymer. The melting temperature of the polymer and composite matrix also increases. Although crystallinity is inhibited in the LD133A sample with the addition of fibers, it can be recovered through annealing. Annealing does not seem to appreciably change the fraction of overall crystallinity for HD7760 but it does increase the melting point significantly. For the HD77560 composite, the melting point and fraction of crystallinity increase.

Annealing seems to significantly affect the shape of the DSC curve through the first heating cycle, i.e. the state of crystallinity is markedly changed. On the first heating, the un-annealed sample has a wide peak. The annealed sample has a narrower peak that is deeper. A second lower temperature peak begins to appear that is much smaller in area. It would seem that the un-annealed sample has a distribution of crystal sizes and this is the origin of the wider, shallower peak. Annealing allows the crystals an opportunity to perfect themselves and grow. This narrows the crystal size distribution and, in fact, two narrow populations of crystals arise, each corresponding to a melting peak. There is a large population of similarly sized crystals at the higher melting temperature and a very small population of similarly sized crystals at the lower melting temperature. Xie et al. [29] observe similar behavior when annealing HDPE and LDPE and term this 'thermal fractionation'. Different sized crystals are related to different packings among chain segments. Analysis of the second heating cycle shows that the small lower temperature peak disappears. The melting peak of the second heating

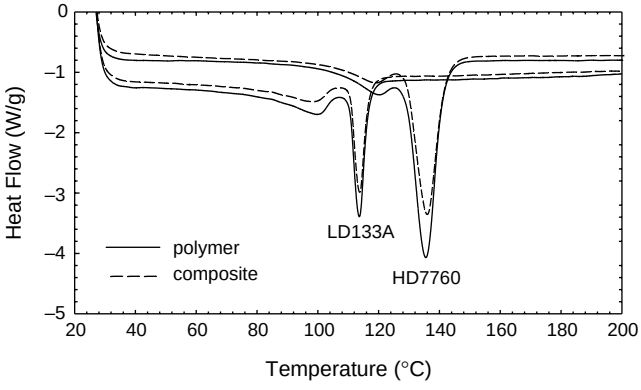

Fig. 4. Effect of annealing on LD133A and HD7760 polymers and composites as shown by DSC first heating curve.

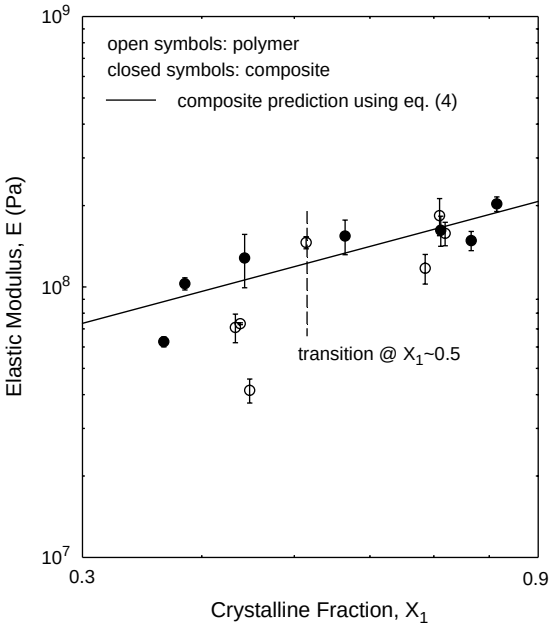

Fig. 5. Elastic modulus, E, of polymers and composites plotted as a function of polymer crystallinity, X_1.

cycle looks very similar to the melting peak of the un-annealed sample so the first heating cycle returns the annealed sample back to its original crystalline state.

3.3. Effect of polymer crystallinity on properties

Figs. 5 and 6 show the physical properties of the polymers and composites as a function of polymer matrix crystallinity after the first heating cycle, X_1. X_1 represents the state of crystallinity following processing and the solid-state properties depend on this parameter. The individual samples can be identified by cross-referencing the X_1 values in Figs. 5 and 6 with Table 2. Fig. 5 shows that E increases with polymer crystallinity up to about $X_1 \sim 0.5$, when the properties of the polymer and composite are comparable for a given value of X_1. In Fig. 6, the peak stress, σ_p, follows a similar trend. However, at $X_1 > 0.5$, σ_p of the composites can be lower than that of the polymers.

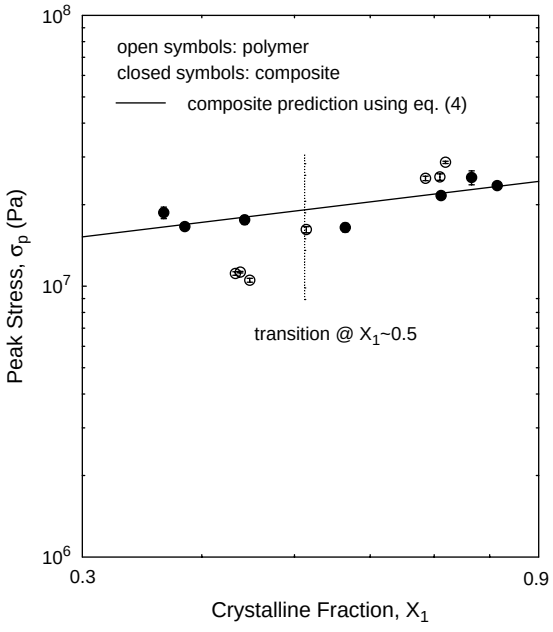

Fig. 6. Peak stress, σ_p, of polymers and composites plotted as a function of polymer crystallinity, X_1.

Above $X_1 \sim 0.5$, the fibers enhance polymer crystallinity in the composites. For a given crystallinity value, the modulus of the polymers is comparable to the modulus of the composites, even though the composites have more crystallinity and a fiber phase. Above $X_1 \sim 0.5$, the peak stress of the polymers appears to be higher than the composites, even though the composites have more crystallinity in the matrix phase and a fiber phase. This would indicate that there is minimal fiber/polymer interaction for the highly crystalline polymers. Fig. 7(a) and (b) show SEM micrographs of the LD133A and HD7760 tensile bar fracture surfaces, respectively. LD133A adheres to the keratin fiber while there is a void around the keratin fibers in the HD7760 composites. It appears that the high crystallinity causes the polymer to contract off of the fiber surface

Fig. 7. Scanning electron micrograph of: (a) LD133A/20 wt% 0.1 cm feather fiber composite and (b) HD7760/20 wt% 0.1 cm feather fiber composite.

upon cooling from the melt. There does not appear to be an issue of wetting because LD133A and HD5502SA have similar MFI values, which would imply similar viscosities, and therefore would wet the fibers similarly at the same temperature. LLDPE 2037 has the highest MFI and therefore the lowest viscosity but still does not benefit from reinforcement from the fibers and this polymer would be expected to wet the fibers the best. Chemical compatibility is not an issue because all of the polymers are PE and all of the fibers are the same keratin fiber.

Below a crystallinity value of about $X_1 \sim 0.5$, the fibers significantly increase E and σ_p. For the composites in the region $X_1 < 0.5$, the fibers inhibit crystallinity but the modulus and peak stress are still much higher than the higher crystallinity pure polymers. So the fibers carry applied load. Annealing the lower crystallinity PE's restores not only the crystallinity, but the properties of the annealed samples are increased over the un-annealed samples. Annealing at 2–10 °C below the melting point of the polymer has proven to be an effective method to increase polymer physical properties [29].

3.4. Modeling composite properties as a function of matrix crystallinity

The physical properties of semi-crystalline polymers reinforced with fibers are derived from both the crystallinity in the matrix phase, the intrinsic physical properties of the fibers, and the interaction between the polymer and fiber. The crystallinity in the matrix phase depends on the processing method and the presence of fibers. Therefore, a micromechanical model that more appropriately describes the contribution from the crystallinity and how the crystallinity is affected by the presence of fibers is developed.

Beginning with the crystallinity of the pure polymer, $X_{1,p}$ ($m_f = 0$ in Eq. (1)), and the composite matrix, $X_{1,m}$ ($m_f \neq 0$ in Eq. (1)), obtained from DSC, the density of the composite matrix, ρ_m, can be found from

$$\rho_m = \left(\frac{X_{1,m}}{\rho_c} + \frac{1 - X_{1,m}}{\rho_a} \right)^{-1} \tag{2}$$

where $\rho_c = 1.0111$ g/cm^3 and $\rho_a = 0.8621$ g/cm^3 are the densities of 100% crystalline and amorphous PE, respectively [30]. Coincidentally, using $X_{1,p}$ in Eq. (2) to compute the polymer density gives values very close to the densities of the PE's reported by the manufacturers and listed in Table 1. The volume fraction of fiber, ϕ_f, can be found from ρ_m

$$\phi_f = \frac{\frac{m_f}{\rho_f}}{\frac{m_f}{\rho_f} + \frac{m_m}{\rho_m}} \tag{3}$$

where m_m is the mass fraction matrix and ρ_f is the fiber density of 0.89 g/cm^3 [24]. To predict the composite properties as a function of matrix crystallinity and volume fraction fiber, a 'rule of mixtures' model is used based on volume fraction of fiber and matrix, $\phi_f + \phi_m = 1$

$$E_c = k\phi_f E_f + \phi_m E_m \tag{4}$$

where f denotes fiber, m denotes matrix and k is a fitting parameter that describes fiber aspect ratio, orientation of the fibers relative to the loading direction, and fiber/polymer adhesion in the solid state. All of the fibers used are the same dimensions and the composites are all processed the same way so k is only a function of fiber/polymer adhesion in the solid state. The modulus value used for the fibers, E_f, is 5 GPa [24]. From the thermal properties study, it is already known that if the pure polymer modulus, E_p, is used for the value of E_m it will not be accurate because the presence of the fibers changes the polymer matrix crystallinity and, therefore, the properties. Upon crystallizing from the melt, a new crystallinity state is reached that changes the matrix modulus from E_p to E_m. E_m is found from E_p and the DSC data by using

$$E_m = E_p \left[\frac{X_{1,m}}{X_{1,p}} \right] \tag{5}$$

which can then be inserted into Eq. (4) along with values for ϕ_f obtained from $X_{1,m}$ and m_f. Similarly, the peak stress of the composite, $\sigma_{p,c}$, can be found by inserting the stress values into Eqs. (4) and (5) with a fiber tensile stress value of $\sigma_f = 200$ MPa used [24]. The lines in Figs. 5 and 6 show the composite properties prediction using this approach. In Fig. 8, the k values used are plotted as a function of the composite matrix crystalline fraction, $X_{1,m}$. Fig. 8 shows that the more matrix crystallinity, the less polymer adhesion to the fibers in the solid state. In addition, the peak stress is a stronger indicator of polymer/fiber adhesion than the modulus. Although the σ_p curve is fit to a first order

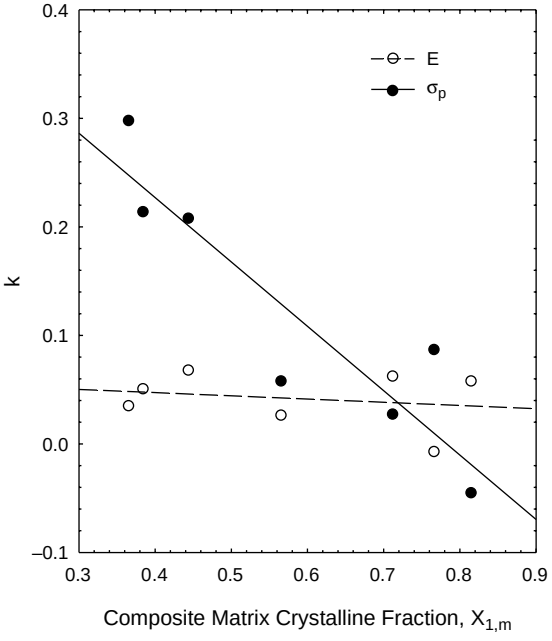

Fig. 8. Adhesion parameter, k, plotted as a function of polymer composite matrix crystallinity, $X_{1,m}$.

polynomial, there is a large drop in k at around $X_{1,m} \sim 0.5$, concurrent with the physical and thermal property data.

4. Conclusions

In this paper, fiber/polymer physical interactions are studied by varying polymer chain architecture and composite processing conditions. These physical interactions occur in the melt state and reflect a change in crystallinity upon cooling from the melt. The physical interactions also occur in the solid state and manifest as a change in the adhesion of the polymer to the fiber. The chemical nature of the polymers remains constant and, therefore, chemical interaction between the polymers and fibers is constant. It is found that polyethylenes with a crystalline fraction less than about 0.5 adsorb onto keratin feather fibers and remain adsorbed after melt processing and through subsequent cooling. The strong fiber/polymer interactions show that the low crystallinity polyethylenes are reinforced by the keratin feather fibers. In contrast, high crystallinity polyethylenes, i.e. with crystalline fraction greater than about 0.5, are not reinforced by keratin feather fiber. Although there may be interaction between the polymer chains and fibers during processing in the melt state, these interactions are not strong or do not persist upon cooling from the melt. This may show a method to compatibilize fiber composites through a physical, rather than chemical, i.e. coupling agent, mechanism by controlling the processing [18] to induce lower crystallinity around the fibers or by treating the fibers with a lower crystallinity polymer.

References

[1] Kuan H-C, Huang J-M, Ma C-CM, Wang F-Y. Processability, morphology and mechanical properties of wood flour reinforced high density polyethylene composites. Plast Rubber Compos 2003;32:122–6.

[2] Colom X, Carrasco F, Pages P, Canavate J. Effects of different treatments on the interface of HDPE/lignocellulosic fiber composites. Compos Sci Technol 2003;63:161–9.

[3] Singleton ACN, Baillie CA, Beaumont PWR, Peijs T. On the mechanical properties, deformation and fracture of a natural fibre/recycled polymer composite. Composites Part B 2003;34:519–26.

[4] Wambua P, Ivens J, Verpoest I. Natural fibres: can they replace glass in fibre reinforced plastics? Compos Sci Technol 2003;63:1259–64.

[5] Cantero G, Arbelaiz A, Mugika F, Valea A, Mondragon I. Mechanical behavior of wood/polypropylene composites: effects of fibre treatments and ageing processes. J Reinf Plast Compos 2003;22:37–50.

[6] Jayaraman K. Manufacturing sisal–polypropylene composites with minimum fibre degradation. Compos Sci Technol 2003;63:367–74.

[7] Maldas D, Kokta BV. Composite molded products based on recycled polypropylene and woodflour. J Thermoplast Compos Mater 1995;8:420–34.

[8] Bledzki AK, Gassan J. Composites reinforced with cellulose based fibres. Prog Polym Sci 1999;24:221–74.

[9] Chawla KK. Composite materials. New York: Springer; 1987.

[10] Sreekala MS, Thomas S. Effect of fibre surface modification on water-sorption characteristics of oil palm fibres. Compos Sci Technol 2003;63:861–9.

[11] Joseph PV, Joseph K, Thomas S, Pillai CKS, Prasad VS, Groeninckx G, et al. The thermal and crystallization studies of short sisal fibre reinforced polypropylene composites. Composites Part A 2003;34:253–66.

[12] Rana AK, Mandal A, Bandyopadhyay S. Short jute fiber reinforced polypropylene composites: effect of compatibiliser, impact modifier and fiber loading. Compos Sci Technol 2003;63:801–6.

[13] Murayama-Arai K, Takahashi R, Yokote Y, Akahane K. Amino acid sequence of feather keratin from fowl. Eur J Biochem 1983;132:501–7.

[14] Martinez-Hernandez AL, Velasco-Santos C, de Icaza M, Castano VM. Grafting of methyl methacrylate onto natural keratin. e-Polymers 2003;016:1–11.

[15] Tsukada M, Shiozaki H, Freddi G, Crighton JS. Graft copolymerization of benzyl methacrylate onto wool fibers. J Appl Polym Sci 1997;64:343–50.

[16] Bullions TA, Gillespie RA, Price-O'Brien J, Loos AC. The effect of maleic anhydride modified polypropylene on the mechanical properties of feather fiber, kraft pulp, polypropylene composites. J Appl Polym Sci 2004;92:3771–83.

[17] Thomason JL, van Rooyen AA. The transcrystalline interphase in thermoplastic composites. In: Ishida H, editor. Controlled interphases in composite materials. New York: Elsevier; 1990.

[18] Gao S-L, Kim J-K. Cooling rate influences in carbon fibre/PEEK composites. Part 1. Crystallinity and interface adhesion. Composites Part A 2000;31:517–30.

[19] Zafeiropoulos NE, Baillie CA, Matthews FL. An investigation of the effect of processing conditions on the interface of flax/polypropylene composites. Adv Compos Lett 2001;10:293–7.

[20] Van Dommelen JAW, Brekelmans WAM, Baaijens FPT. Multiscale modeling of particle-modified polyethylene. J Mater Sci 2003;38:4393–405.

[21] Bartczak Z, Argon AS, Cohen RE, Weinberg M. Toughness mechanism in semi-crystalline polymer blends: I. High-density polyethylene toughened with rubbers. Polymer 1999;40:2331–46.

[22] Bartczak Z, Argon AS, Cohen RE, Weinberg M. Toughness mechanism in semi-crystalline polymer blends: II. High-density polyethylene toughened with calcium carbonate filler particles. Polymer 1999;40:2347–65.

[23] Gassner G, Schmidt W, Line MJ, Thomas C, Water, RM. Fiber and fiber products from feathers. US Patent No. 5,705,030; 1998.

[24] Barone JR, Schmidt WF. Polyethylene reinforced with keratin fibers obtained from chicken feathers. Compos Sci Technol 2005;65:173–81.

[25] Schuster J. Polypropylene reinforced with chicken feathers. 14th International Conference on Composite Materials, San Diego, CA, July 14–18; 2003.

[26] Dweib MA, Hu B, O'Donnell A, Shenton HW, Wool RP. All natural composite sandwich beams for structural applications. Compos Struct 2004;63:147–57.

[27] Kuroda MMH, Scott CE. Initial dispersion mechanisms of chopped glass fibers in polystyrene. Polym Compos 2002;23:395–405.

[28] Wunderlich B. Macromolecular physics. vol. 3. New York: Academic Press; 1980.

[29] Xie Y, Zhang Q, Fan X. Study of the fine crystalline structure of polyethylenes via annealing and thermal fractionation. J Appl Polym Sci 2003;89:2686–91.

[30] McCrum NG, Buckley CP, Bucknall CB. Principles of polymer engineering. New York: Oxford University Press; 1992.